

# FLEXNN: A Dataflow-aware Flexible Deep Learning Accelerator for Energy-Efficient Edge Devices

Arnab Raha, Deepak A. Mathaikutty, Soumendu K. Ghosh and Shamik Kundu\*

Advanced Architecture Research, NPU IP, CGAI (CCG), Intel Corporation, Santa Clara, CA, USA

Email: {arnab.raha, deepak.a.mathaikutty, soumendu.ghosh, shamik.kundu}@intel.com

**Abstract**—This paper introduces FLEXNN, a Flexible Neural Network accelerator, which adopts agile design principles to enable versatile dataflows, enhancing energy efficiency. Unlike conventional convolutional neural network accelerator architectures that adhere to fixed dataflows (such as input, weight, output, or row stationary) for transferring activations and weights between storage and compute units, our design revolutionizes by enabling adaptable dataflows of any type through software configurable descriptors. Considering that data movement costs considerably outweigh compute costs from an energy perspective, the flexibility in dataflow allows us to optimize the movement per layer for minimal data transfer and energy consumption, a capability unattainable in fixed dataflow architectures. To further enhance throughput and reduce energy consumption in the FLEXNN architecture, we propose a novel sparsity-based acceleration logic that utilizes fine-grained sparsity in both the activation and weight tensors to bypass redundant computations, thus optimizing the convolution engine within the hardware accelerator. Extensive experimental results underscore a significant enhancement in the performance and energy efficiency of FLEXNN relative to existing DNN accelerators.

**Index Terms**—Deep neural network accelerator, flexible data flow, sparsity acceleration, energy efficiency.

## I. INTRODUCTION

The landscape of machine learning is experiencing an unprecedented surge, with a multitude of artificial intelligence (AI) networks proposed alongside the development of numerous hardware platforms dedicated to accelerating inference tasks. As the field progresses, the complexity of neural networks continues to grow, resulting in the handling of vast amounts of tensor data that exhibit diverse shapes and dimensions across different layers of existing networks. Moreover, with the continuous introduction of new models, the dimensions of these tensor data are in constant flux. Consequently, there is a pressing need to engineer hardware accelerators with the flexibility to efficiently process network layers of varying dimensions [1], [2].

Furthermore, the proliferation of edge devices, including wearables, smart cameras, smartphones, and surveillance platforms, underscores the importance of energy efficiency in the design of neural network accelerators [3]. Given that tensor data processing involves traversing multiple levels of memory hierarchy, minimizing data transfer while maximizing data reuse and resource utilization emerges as critical imperatives to

improve the energy efficiency of Deep Neural Network (DNN) accelerators [4].

However, the prevailing accelerators for DNN execution, such as Eyeriss [5] and TPU [6], typically adopt custom memory hierarchies and fixed dataflows. These architectures dictate the sequence in which the tensor data for the activations and weights are moved to processing units to execute the tensor operations for each layer of the network. Although effective, these approaches may not fully exploit the potential for energy efficiency optimization inherent in more flexible hardware designs. Therefore, there is a growing interest in exploring novel architectures and strategies that can better adapt to the evolving demands of neural network inference while simultaneously improving energy efficiency across a range of edge devices and applications.

The energy consumption for each layer in neural network inference is heavily influenced by the movement of data across the memory hierarchy and the level of reuse within the processing units. Previous studies have endeavored to characterize energy efficiency through analytical models while stressing the importance of enabling flexibility in scheduling tensors of varying dimensions [7]. This flexibility involves optimizing the ordering, blocking, and partitioning of tensors to maximize reuse from the innermost memory hierarchy, where the energy cost per unit of data moved is minimized. However, most existing DNNs, such as ResNet, YOLO, VGG, and GoogLeNet, comprise tens to hundreds of layers, each with different preferences for scheduling to achieve energy optimality. Fixed-schedule DNN accelerators can only offer optimal data reuse and resource utilization for a subset of DNN layers, thus limiting overall energy efficiency. Moreover, these accelerators exhibit strong network dependencies, posing challenges in adapting to the rapidly evolving landscape of DNNs. Existing DNN accelerator designs from both industry and academia predominantly employ fixed schedules, such as weight stationary (WS), output stationary (OS), non-local reuse (NR), and row stationary (RS) [8], [9]. The fixed dataflow characteristic of these accelerators originates from their tensor data distribution modules, which perform addressing to on-die storage, data transfer to processing engine arrays, and data storage to SRAM banks in a predetermined manner.

As a result, existing accelerators lack the flexibility to implement different schedules (*i.e.*, dataflows), and while software-based solutions on general-purpose CPUs and GPUs can reshape and load tensor data, fixed-function accelerators do

\*Shamik Kundu contributed to this work during his internship in the Advanced Architecture Research Group during summers '22 and '23. He is currently a PhD student at UT Dallas. (Email: [shamik.kundu@utdallas.edu](mailto:shamik.kundu@utdallas.edu))

not support such flexibility. FPGAs, although offering flexibility, cannot alter the hardware configuration during execution from one layer to another of a DNN.

In contrast to previous approaches, this paper proposes a dataflow-aware flexible DNN accelerator that leverages schedule information from DNN layers to adapt tensor data shape and internal compute configuration on a per-layer basis. This enables the compiler to configure the DNN accelerator optimally for handling tensor operations based on tensor dimensions. The key advantage of our proposed accelerator design lies in its ability to switch among multiple schedules based on layer characteristics, thereby minimizing memory accesses for a given tensor operation and resulting in significant energy savings at the accelerator level.

To further enhance performance and increase energy efficiency in the accelerator, we capitalize on the inherent sparsity inherent in DNNs. Due to the nature of DNNs, the weights associated with the network are often “sparse,” meaning that they contain a significant number of zeros generated during the training phase [10], [11]. These zero-valued weights do not contribute to the accumulation of partial sums during multiply-and-accumulate (MAC) operations. Additionally, highly sparse weights cause activations to become sparse in subsequent layers of the DNN after passing through non-linear activation functions like ReLU. Furthermore, network quantization for edge device inference also results in a high number of zeros in both weights and activations. The unstructured fine-grained sparsity in weights and activations offers potential for improved energy efficiency and processing speed in two ways: (1) MAC computation can be gated or skipped, and (2) weights and activations can be compressed to reduce storage and data movement. The former reduces energy consumption, while the latter reduces both energy consumption and processing cycles. However, designing DNN accelerators to harness these benefits from sparsity is challenging due to irregular access patterns, workload imbalances, and under-utilization of MAC-based processing elements [12]. Hence, in this paper, we develop a novel sparsity acceleration logic capable of skipping zero-valued compression while simultaneously identifying non-zero elements in both activation and weight tensors. This will facilitate the implementation of an efficient convolution engine in the hardware accelerator at the edge, enabling efficient utilization of resources and enhancing overall performance and energy efficiency.

In summary, in this paper, we introduce FLEXNN, a **Flexible** Neural Network accelerator, designed with agile principles to support versatile dataflows, thereby enhancing energy efficiency. Recognizing that data movement costs significantly outweigh compute costs in terms of energy consumption, the flexibility in dataflow enables us to optimize data transfer per layer, leading to minimal data movement and reduced energy consumption, an advantage not achievable in fixed dataflow architectures. Additionally, to further boost throughput and reduce energy consumption within the FLEXNN architecture, we propose an innovative sparsity-based acceleration logic. This logic harnesses fine-grained sparsity in both activation and weight

tensors to bypass redundant computations, effectively optimizing the convolution engine within the hardware accelerator. This paper makes the following contributions.

- This paper introduces a novel DNN accelerator, FLEXNN, designed to be sensitive to dataflow, offering flexibility by integrating DNN layer scheduling insights. By dynamically adjusting tensor data shape and the internal compute configuration for each layer, the accelerator allows the compiler to optimize its performance in handling tensor operations, tailoring its configurations based on tensor dimensions for diverse neural network architectures.
- We introduce a novel sparsity acceleration logic that capitalizes on the unstructured fine-grained sparsity present in incoming activation and weights, thereby expediting inference execution within the DNN accelerator. Data are maintained in a zero-compressed format to mitigate storage and data movement expenses. Weights and activations are mapped while considering sparsity to enhance reuse, thereby enhancing overall performance.
- Extensive experimental evaluations conducted on six distinct DNNs spanning both classification and detection tasks highlight the transformative impact of our accelerator. Specifically, our architecture showcases substantial improvements over fixed-schedule accelerators for ResNet101 and YOLOv2, demonstrating up to 77% and 62% energy reduction over Eyeriss and TPU, respectively. Furthermore, our accelerator achieves notable sparsity improvements for four additional DNNs, namely ResNet50, MobileNetV2, GoogLeNet, InceptionV3. Across these benchmarks, FLEXNN achieves a speedup of  $2.0\times$ – $2.7\times$  over dense accelerators and  $1.3\times$ – $1.8\times$  over semi-sparse accelerators with weight-sparsity support. Sparsity support also provides  $1.9\times$ – $2.5\times$  and  $1.3\times$ – $1.7\times$  improvement in energy efficiency compared to dense and weight-sided accelerator. These results underscore the profound impact of our accelerator in enabling efficient execution of sparse and compact DNNs, significantly enhancing both speed and energy consumption metrics.

The remainder of the paper is organized as follows. Section II delineates the need for a flexible dataflow and an efficient two-sided sparsity acceleration logic. Section III describes the microarchitectural details of the proposed FLEXNN accelerator. Section IV presents the experimental setup followed by the results in Section V. The prior art in this domain is outlined in Section VI. Finally, Section VII concludes the paper.

## II. MOTIVATION

In this section, we delve into the fundamental motivations driving the design and development of our accelerator architecture, focusing on two key aspects: the paramount importance of flexibility and the critical need for efficient sparsity acceleration. By addressing these critical considerations, our accelerator aims to revolutionize the landscape of deep learning hardware, offering unparalleled versatility and performance across a wide range of neural network models and applications. We explore

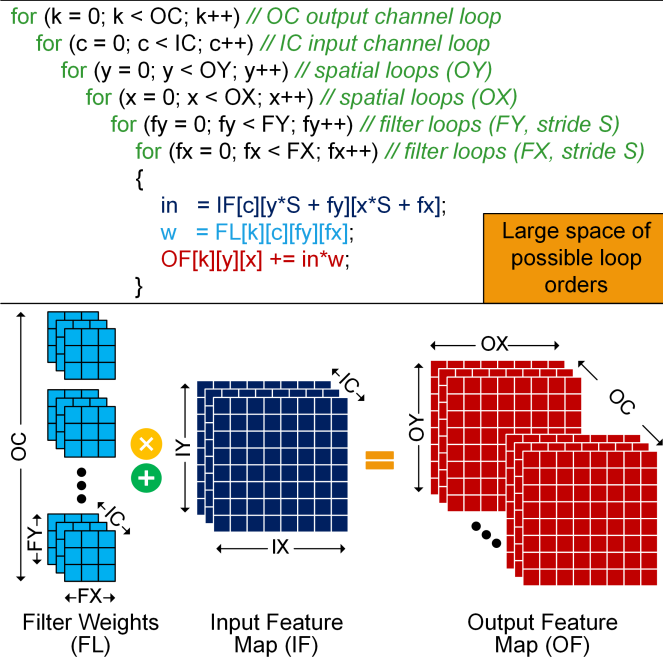


Fig. 1: Illustration of multi-loop tensor processing during convolution operation in DNN.

how these foundational principles drive innovation and shape the architectural decisions that lead to the design of FLEXNN.

### A. Importance of flexibility

Numerous DNN accelerators utilize spatial architectures comprised of arrays of processing elements (PEs) alongside local storage like register files (RFs) for those PEs, as well as external storage such as SRAM banks. In inference tasks, trained weights, or filters (FL), must be loaded into PE arrays from storage sources like DRAMs and SRAM buffers. Input images, referred to as input activations or feature maps (IFs), are also transferred into PE arrays, where MAC operations occur across multiple input channels (ICs) between activations and weights, generating output activations (OFs). Multiple sets of weight tensors (OCs) are commonly used against a specific set of activations to produce an output tensor volume. Finally, a non-linear function (*e.g.*, ReLU) is applied to the output activations, which then become the input activations for the subsequent layer. The tensor processing involved in a convolution operation, as shown in Fig. 1, showcases convolution layers comprising seven nested loops. These layers generate an output tensor, OF map, from multiple kernel feature maps, FLs, operating on one or more input tensors, IF map. Each point in the output volume undergoes a MAC operation during the calculation. For instance, a  $1 \times 1$  convolution layer, such as the second convolution layer in ResNet50, illustrates IF map dimensions of  $IX = 56$ ,  $IY = 56$ ,  $IC = 64$ , and the filters dimensions of  $FX = 1$ ,  $FY = 1$ ,  $IC = 64$ ,  $OC = 256$ . These dimensions convolve (with a batch size of  $ON = 1$ ) to produce an OF map with dimensions  $OX = 56$ ,  $OY = 56$ ,  $OC = 256$ , accompanied by appropriate padding values.

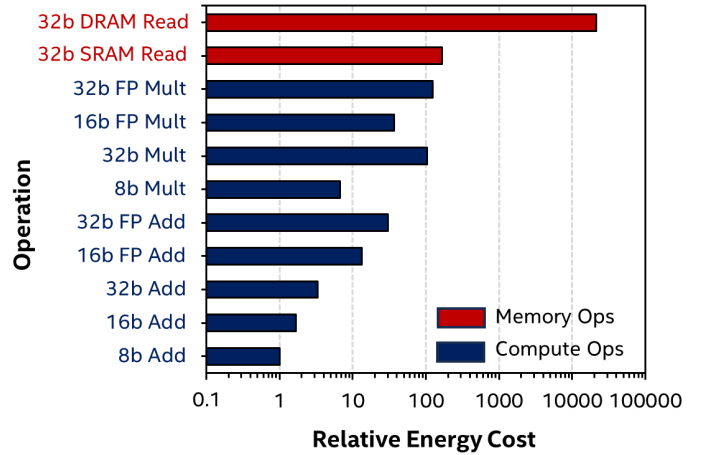


Fig. 2: Relative energy costs of different compute and memory operations at various precisions in 45 nm technology [14]. Note that x-axis is in logarithmic scale.

The dimensions of the input tensor undergo changes as they transition from one layer to another within a DNN and across various DNNs. Consequently, the development of flexible hardware accelerators becomes crucial to maintaining high utilization of compute units across network layers with arbitrary dimensions. Attempting to map various tensor dimensions to a fixed PE array with a consistent tensor mapping pattern can lead to decreased array utilization. To improve performance and energy efficiency, it is imperative to minimize data movement by maximizing data reuse from local memory and improving resource utilization. This optimization is particularly vital, as the cost of memory accesses often exceeds that of computing, as illustrated in Fig. 2. Numerous existing DNN accelerators, such as Eyeriss [12], TPU [13], and SCNN [10], implement novel memory hierarchies and fixed dataflows, influencing the movement of tensors for activations and weights within the processing units and the workload assigned to each PE. A fixed dataflow constrains the types of data movement across the memory hierarchy, limiting the degree of reuse within processing units. The movement of input activations (IFs), weights (FLs), and partial sums, as well as the order of reuse, directly impact the energy consumption for each layer. In the literature [7], inference accelerators are classified into input stationary, weight stationary, output stationary, and row stationary based on the dataflow. The data reuse scheme is based on loop order, loop blocking, and partitioning for tensor processing, collectively called a “schedule”, as depicted in Fig. 3. This schedule is described in relation to the dimensions of the tensors in a convolutional neural network. The loop order dictates the relative order of  $IX$ ,  $IY$  (spatial), and  $IC$  dimensions for activations and  $FX$ ,  $FY$ ,  $IC$ ,  $OC$  dimensions for filters when loading these data into the accelerator. Moreover, loop partitioning dictates how the overall convolution operation is distributed among the PEs in the PE array, while loop blocking governs the allocation of multiple points in each dimension to the same PE.

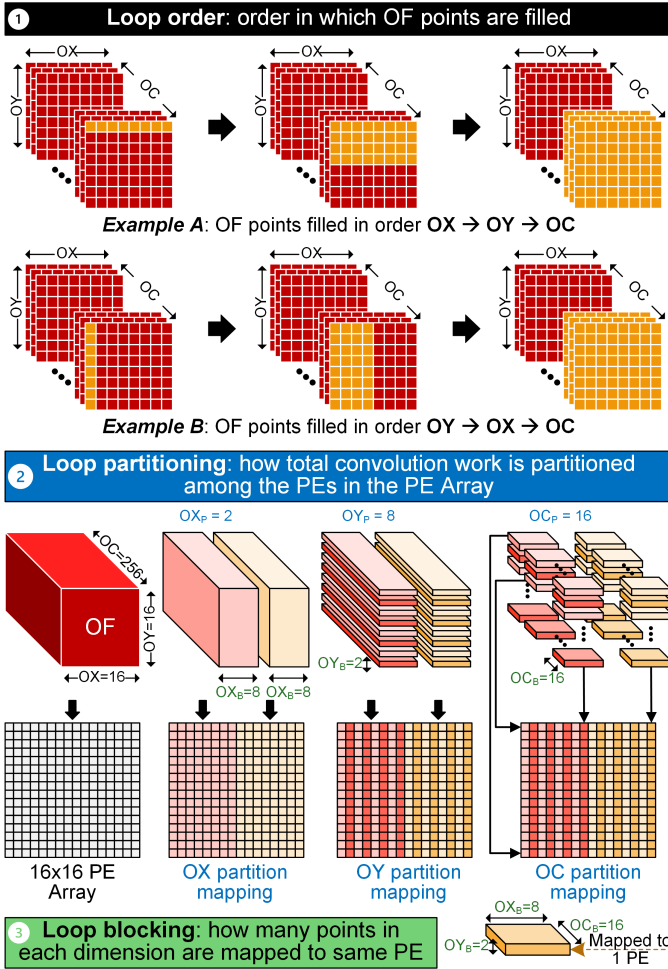


Fig. 3: Illustration of (1) loop order, (2) loop partitioning and (3) loop blocking — referred to collectively as scheduling — for optimizing data loading and distribution in the accelerator.

All existing inference engines operate with fixed loop orders, blocking, and partitioning for convolution operations. Consequently, each accelerator can only execute a single predetermined dataflow, where the data remain stationary in only one aspect. Various schedules require that IFs, FLs, and OFs/partial sums be mapped and accessed from local register file (RF) storage differently based on the type of schedule being computed. For instance, in the Input Stationary (IS) scenario, a single point within the IF RF must undergo multiplication and accumulation against multiple points in the FL RF. The frequency of this repetition of operations varies on the basis of the schedule. Similarly, in the Weight Stationary (WS) situation, a single point within the FL RF must be multiplied and accumulated against multiple points in the IF RF. Lastly, for Output Stationary (OS) schedules, the same partial sum in the OF RF must be retained and used to accumulate the results of multiplication between distinct IF and FL RF points over multiple cycles. Additionally, when the size of the SRAM imposes limitations on the number of IC points that can be stored, incomplete OF points in the form

of partial sums must be transferred to a higher-level memory hierarchy for subsequent retrieval into PE RFs to complete the OF computation across all input channels.

Previous research aimed at characterizing the energy efficiency of DNN accelerators by constructing analytical models underscores the need to introduce flexibility in scheduling tensor operations of various dimensions to maximize reuse from the innermost memory hierarchy, where the energy cost per unit of data moved is minimized [7]. Vision networks such as ResNet, YOLO, and VGG consist of tens to hundreds of layers, each favoring different dataflows to achieve optimal energy efficiency. In contrast, fixed dataflows can only cater to optimal data reuse and resource utilization for a limited subset of DNN layers. The proposed tensor data computing PE array offers a practical solution to address the flexibility challenge with minimal hardware overhead. Realizing a flexible dataflow accelerator requires a dataflow-aware tensor distribution unit capable of utilizing layer-specific optimal schedules and dataflow information to distribute data to the array. Moreover, the accelerator should inherently support flexible mapping and execution of these data within each PE.

**Motivation 1:** *It is important to develop a flexible dataflow in order to minimize data movement and maximize reuse in the PE array.*

### B. Importance of Sparsity Acceleration

Sparse IFs are inherent in DNNs because of several factors. One primary cause is the prevalent use of the ReLU as an activation function within many DNN architectures. The nature of ReLU to set negative values to zero contributes to sparsity, particularly intensifying in deeper layers, where it often exceeds 90%. Additionally, the rise of auto-encoders and generative adversarial networks (GANs) further accentuates sparsity trends. These network feature decoder layers employ zero insertion techniques to up-sample input feature maps, resulting in more than 75% zeros. In addition, extensive efforts have focused on inducing FL sparsity within DNNs. Various criteria, such as saliency, magnitude, and energy consumption, are employed to determine which weights to prune. As a result, pruned networks exhibit weight sparsity levels of up to 90% [15].

The translation of the sparsity in weights and activations into enhanced energy efficiency and processing speed presents a significant opportunity. However, designing DNN accelerators capable of effectively harnessing these advantages remains a formidable challenge. Computation gating emerges as a promising technique for converting sparsity in both FLs and FLs into energy savings. Its implementation involves recognizing if either the weight or activation is zero and gating the datapath switching and memory accesses accordingly, achieving cost-effective solutions. To optimize throughput while conserving energy, skipping cycles of processing MACs with zero weights or activations becomes desirable. Yet, this necessitates more intricate read logic to locate the next non-zero value without expending cycles on zeros. A natural solution entails maintaining

FLs and IFs in a compressed format indicating the next non-zero location relative to the current one. However, compressed formats, often of variable length, pose challenges for parallel processing across PEs without compromising compression efficiency. Additionally, simultaneous recognition of sparsity in both weights and activations complicates matters, as efficiently ‘looking ahead’ (e.g., skipping non-zero weights when the corresponding activation is zero) proves challenging with many compression formats. The irregularity introduced by such jumps precludes the use of pre-fetching to enhance throughput. Consequently, the control logic for processing compressed data becomes intricate, adding overhead to the PEs. Addressing these complexities is vital to realize the full potential of sparsity in DNN accelerators.

As a result, hardware solutions in this domain have been sparse. For example, Cnvlutin [16] exclusively facilitates skipping cycles for activations without compressing weights, while Cambricon-X [17] lacks the ability to maintain activations in compressed format. Given the intricacies involved in skipping cycles for both weights and activations, existing hardware designed for sparse processing tends to be tailored to specific layer types. For example, EIE [18] is tailored for fully connected (FC) layers, while SCNN [10] is optimized for convolutional (CONV) layers. This specialization underscores the need for further innovation in developing versatile hardware architectures capable of efficiently handling sparsity across various layer types in deep neural networks.

Introducing computation skipping for sparse data fundamentally alters the workload distribution across PEs, as the workload at each PE becomes contingent on sparsity levels. As the count of non-zero values fluctuates across diverse layers, data types, or even within specific regions within the same filter or feature map, it engenders an inherent imbalance in workload distribution across PEs [12]. Consequently, the throughput of the entire DNN accelerator becomes constrained by the PE processing the highest number of non-zero Multiply-Accumulate (MAC) operations. This imbalance inevitably results in reduced PE utilization, thereby impeding the overall efficiency and performance of the DNN accelerator. Addressing this challenge requires innovative strategies to optimize workload distribution and improve PE utilization, thus maximizing the potential benefits of computation skipping for sparse data.

**Motivation 2:** *It is important to develop an acceleration logic that can leverage both unstructured IF and FL sparsity, in zero-compressed format.*

### III. MICROARCHITECTURE DESIGN

This section delineates the array of microarchitecture design decisions and techniques essential for implementing the proposed FLEXNN accelerator.

#### A. Overview of FLEXNN accelerator

The high-level diagram of the DNN accelerator is shown in Fig. 4, illustrating the various microarchitectural components

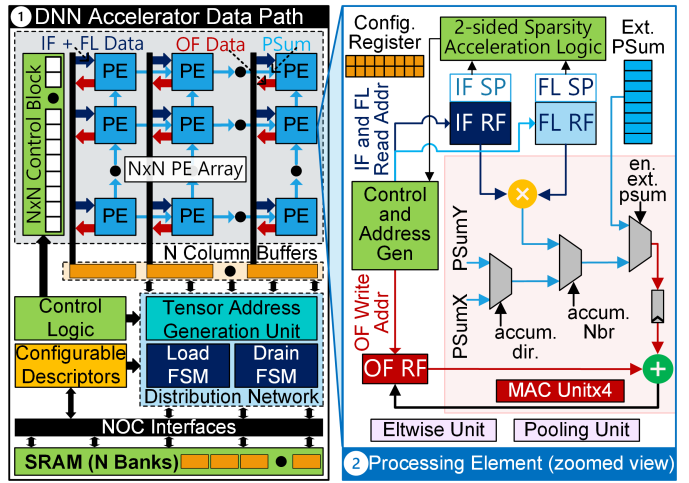


Fig. 4: Top-level schematic of FLEXNN accelerator: (1) Interconnect pathways within the PE array arranged in N columns, data distribution network, control block, and SRAM. (2) Architectural intricacies of the individual PEs showing data storage (IF/FL/OF RF) and sparsity storage (IF/FL SP) and MAC unit.

that facilitate flexible and reconfigurable dataflow. Although the proposed DNN accelerator accommodates any schedule, it remains preferable to configure it according to the optimal schedule for individual layers of the neural network. The optimal schedule is obtained per layer, according to existing research [19], [20]. Leveraging the regularity of DNN computations facilitates efficient data loading into the accelerator and enables flexible convolution mapping based on the optimal schedule. In our design, we assume a three-level memory hierarchy. The first level comprises internal register files within each PE. The second level consists of SRAM, akin to a small L1 cache, storing input operands, output points, and partial sums. The third level encompasses DRAM memory, which is required because of its high capacity to store large amounts of filter weights and spilled OF points. For brevity, we omit DRAM-level implementation specifics and assume that the SRAM’s capacity is sufficient to accommodate all input, intermediate activations, and filter weights. Each memory level gives us the opportunity to reuse data, thus enhancing energy efficiency. The flexible DNN accelerator, capable of supporting  $INT8$ ,  $U8$ ,  $FP16$  and  $BF16$  datatypes, comprises three principal components, elaborated in subsequent sections.

#### B. Versatile Processing Element (VPE) and Flexible Processing Element Array (FPA)

The Versatile Processing Element (VPE) serves as the fundamental computational unit within the proposed FLEXNN accelerator, tasked primarily with executing MAC operations between IF and FL points [21]–[23]. VPE also facilitates the accumulation of internal/ external partial sums (psums). In the context of the flexible accelerator, the VPE optimizes the reuse of IF/FL/OF data and selects the most suitable compute template based on the optimal schedule for each layer. The

Flexible Processing Element Array (FPA) comprises an  $N \times M$  array of VPEs, with the array dimension parameterized by design, typically through synthesis parameters. This array can be conceptualized as being arranged into  $M$  columns, each column consisting of  $N$  VPEs. To streamline the control logic, we deliberately adopted a square grid configuration ( $N \times N$ ) for the FPA, using  $N = 16$ , simplifying the associated control mechanisms. Fig. 4.1 illustrates the schematic of the DNN FPA, composed of an array of VPEs that serve as the most important computational units within the DNN accelerator. Each VPE, as demonstrated in Fig. 4.2, features five 1R1W register files (RF) to store input operands (IF and FL), their corresponding sparsity bitmaps, and output values (OF/psum). During a typical MAC operation, the input operands are fetched from the IF and FL RFs, based on the stored bitmaps and the sparsity acceleration logic (described later in Section III-E), and accumulated within the OF RF. Control over read pointers for IF, FL, and OF RFs, as well as the write pointer for OF, is managed using internal counters programmed by the DNN control logic.

The proposed VPE, as demonstrated in Fig. 5 executes computations on IF, FL, and OF/psum tensor data based on the optimal schedule of the current layer. VPE dynamically adjusts the loading and access patterns of the IF, FL and OF/psum tensor data within the PE RFs to maximize reuse of the tensor data. Configuration descriptors are updated at the onset of each convolution layer based on the optimal schedule of the layer, guiding data redirection during load, compute, and drain operations throughout the lifetime of input tensor data. The PE finite-state machine (FSM) incorporates internal counters and logic to generate read and write control signals for the IF, FL, and OF RFs, along with multiplexer control signals to route data from the RFs to the appropriate arithmetic units based on the template ( $V \times V/M \times M$ ) or operation type (MAC/Eltwise) and tensor dimension.

Internal registers within the PE FSM track the total number of PE blocks (or OF/psum points) produced, aiding in addressing IF/FL/OF RFs. Additionally, counters like *ifcount*, *wcount*, and *ofcount* manage the addresses/indexes for IF, FL, and OF RFs, increasing or clearing based on the number of input activations and weights required to calculate each OF point or psum block. The layer schedule determines the type and extent of IF/FL/OF RF data reuse, regulated by internal IF/FL/OF block counters controlling the loading of new IF/FL data and draining OF data each round, as per the layer’s optimal schedule. These internal structures and associated control logic are pivotal to supporting flexible schedules within the VPE. The critical role of VPE in facilitating flexible blocking within the DNN accelerator is realized by dividing the RF into multiple subbanks ( $X$ ) and incorporating  $X$  MACs (e.g.,  $X = 4$ ) alongside multiplexers, allowing the implementation of  $V \times V$ ,  $V \times M$ , and  $M \times M$  templates [24], based on the optimal blocking factor of the layer for dimensions ( $IC_B$ ,  $OC_B$ ), as depicted in Fig. 6.

For specific schedules, the convolution operation can be partitioned to split across multiple VPEs based on ICs. Consequently, DNN computations that generate partial sums (psums) across different sets of ICs for a particular OF point

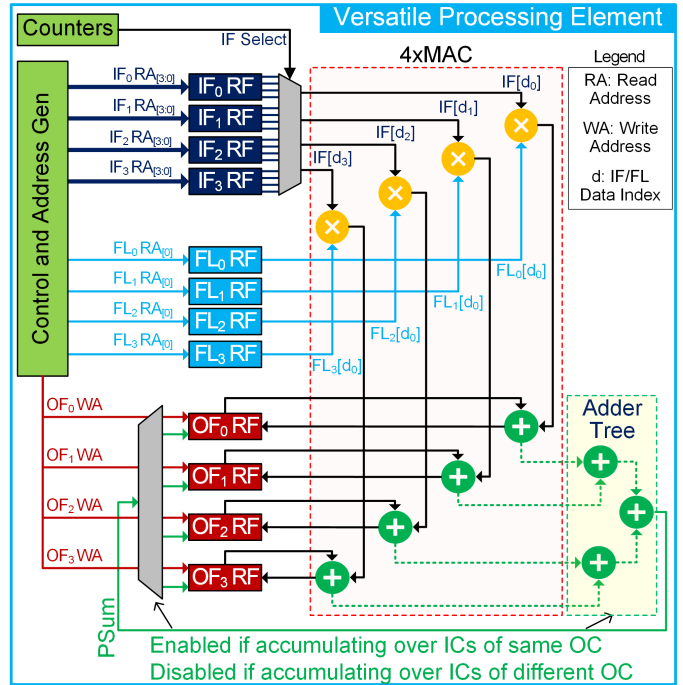


Fig. 5: Microarchitecture of the FLEXNN PE demonstrating inter-connectivity among control units, data register files, and MAC units, alongside support for two accumulation orders.

should be mapped to a single column or row of VPEs. Internal psum accumulation enables accumulation of all ICs partitioned into multiple VPEs to generate the final OF point. The FPA facilitates the transmission of psums formed within the PE to its right or top neighbor, which is essential for the accumulation of internal psum within the FPA. To mitigate wire congestion and routing complexity, interconnections between PEs are restricted to their top and right neighbors. This architectural decision inherently influences how work can be partitioned among different PEs, particularly in the IC dimension.

In certain optimal schedules, all input channels are not accumulated simultaneously. Instead, a portion of the input channel set is initially loaded into the PE RF, and the computed partial sum is extracted to the SRAM (or even DRAM) to be brought back into the PE RFs later when the remaining input channels are accumulated. External partial sum accumulation necessitates a 32-bit wide read and write direct bypass to and from the SRAMs. Sharing arithmetic units for MAC and Eltwise computation, along with multiplexer control logic routing appropriate tensor data into these units, reduces area overhead by enhancing hardware reuse efficiency within the PE. Residual networks like ResNet require element-wise operations, such as the addition of OFs from two convolution layers. To support such operations while maximizing hardware resource reuse, OFs from two different layers are routed into the PE, using existing load and drain paths. The Eltwise field in the programmable descriptor signals an eltwise operation, bypassing the multiply operation within the PE and performing an eltwise addition of the two IF inputs.

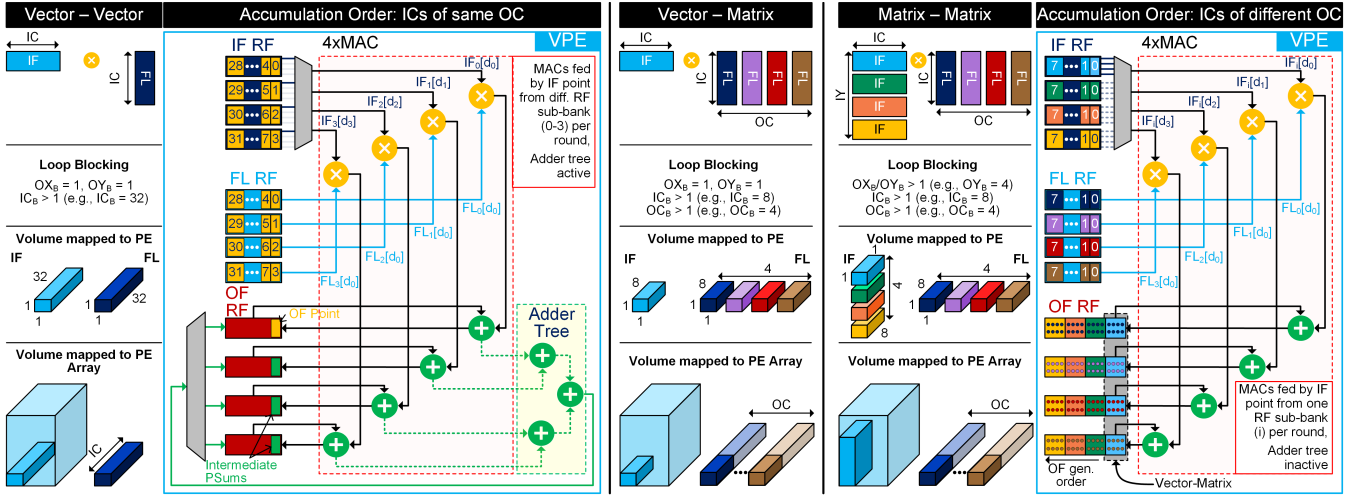


Fig. 6: Vector Processing Element (VPE) accommodating  $V \times V$ ,  $M \times V$ , and  $M \times M$  templates. In  $V \times V$ , accumulation involves Inner Channels (ICs) of the same Output Channel (OC) of weights (FL), while both  $M \times V$  and  $M \times M$  entail accumulation of ICs from different OCs. This illustration presents the dataflow inside the VPE along with loop blocking and partitioning for weights with  $F_X=1$  and  $F_Y=1$ .

### C. Schedule-Aware Flexible Depth Adder Tree (FlexTree)

Our FLEXNN accelerator’s core features a tree-based architecture named FlexTree, designed for partial sum accumulation across numerous PEs within a PE array to generate the final output point [25]. What sets FlexTree apart is its dynamic adjustment of the adder tree’s depth, enabling flexible schedules programmed by the compiler for network layers of diverse dimensions. This hardware enhancement allows the compiler/scheduler to discover highly compute-efficient schedules. FlexTree achieves dynamic reconfiguration of the adder tree depth through software-programmable configuration registers. Unlike existing DNN accelerators where partial sum accumulation occurs by moving partial sums among neighboring PEs, FlexTree’s innovative tree-based architecture significantly enhances partial sum accumulation efficiency (up to  $2.17\times$  speedup). In contrast to state-of-the-art DNN accelerators with fixed schedules and adder tree-based architectures, where the adder tree depth remains fixed at design time, our FlexTree technique offers dynamic reconfiguration capabilities, achieving speedups of up to  $4\times$ – $16\times$ . Thus, our proposed FlexTree architecture enhances compute efficiency by enabling superior partial sum accumulation techniques across a wide range of network layers found in modern DNNs.

Before delving into the FlexTree architecture, it is essential to understand the concept of Input Channel Partition ( $IC_P$ ), similar to OF channel partition as illustrated earlier in Fig. 3.  $IC_P$  denotes how many ICs are assigned to a single PE in the PE array. Consequently, this also denotes the number of PEs that participate in the partial sum accumulation. Let us elucidate  $IC_P$  using an example of 64 input channels. When  $IC_P$  is set to 1, the computation involves only one processing element (PE), denoted PE0. All 64 input channels undergo pointwise multiplication and accumulation within PE0, producing the final

output. In the case of  $IC_P = 2$ , the 64 input channels are evenly divided between PE0 and PE1, with each processing 32 input channels. PE0 accumulates partial sums from input channels 0 to 31, while PE1 accumulates those from channels 32 to 63, forming the final output collectively. Likewise, for  $IC_P = 4$ , the input channels are distributed in PE0, PE1, PE2, and PE3, with each PE handling 16 input channels. These partial sums from the respective set of input channels are accumulated within each PE to generate the final output. Essentially, the product of  $IC_P$  and Input Channel Blocking  $IC_B$  should be equal to  $IC$ .

Fig. 7 illustrates the FlexTree architecture, which receives 16 inputs from the 16 PEs within a column of the PE array in the DNN accelerator.  $IC_P$  supported by the adder tree network ranges from 1 to 16, inclusively. Even if  $IC_P = 2$ , the output of the computation must still pass through the adder tree network before yielding the final OF output. This ensures a reduction in hardware overhead by simplifying hardware design and achieving uniformity across all  $IC_P$  values. It is noteworthy that our FlexTree architecture can accommodate  $IC_P$  values that are not powers of 2 by inputting zeros into the FlexTree network of PEs that do not align with powers of 2. Each module marked with a ‘+’ sign comprises both the INT8 adder and the FP16 adder to support convolution layers of different precision [26]. Depending on the input precision (INT8 vs. FP16), the partial sum output from the PEs is routed to the appropriate hardware resource within FlexTree. In Fig. 7, for  $IC_P$  values of [1, 2], the flops [A, B, C, D, E, F, G, H] at level 1 serve as the final OF output tap points. For  $IC_P = [4]$ , the flops [I, J, K, L] at level 2 act as the final OF output tap points. Similarly, for  $IC_P$  values of [8] and [16], the flops [M, N] at level 3 and [O] at level 4, respectively, serve as the final OF output tap points. The total number of FlexTree output tap points varies for different  $IC_P$  values. Therefore,

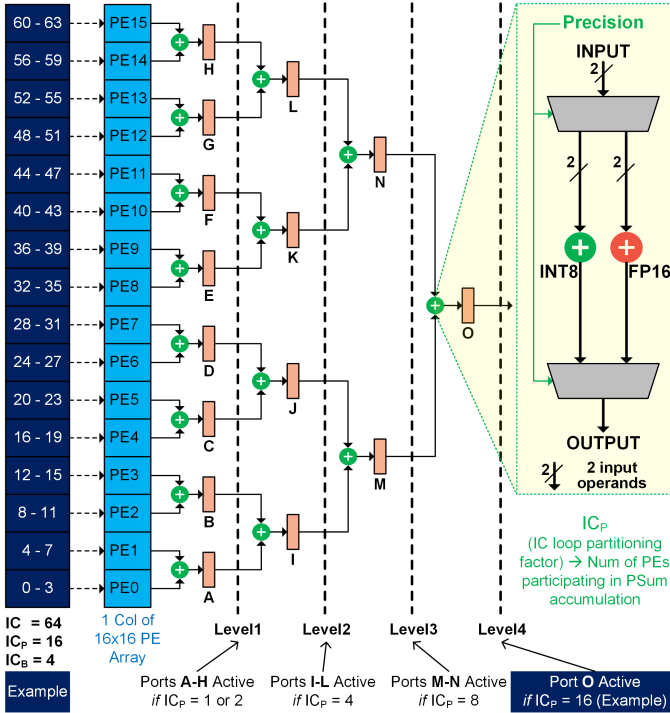


Fig. 7: FlexTree architecture details with illustration using 64 input channels and 16 input channel partition factor.

for  $IC_P$  values of [1, 2, 4, 8, 16], the total number of FlexTree output tap points is [8, 8, 4, 2, 1], respectively. To simplify the extraction of final OF points from the FlexTree module into the drain module, we allow a maximum of 4 output feature map (OF) points to be extracted from the FlexTree output. The illustration shown in the figure assumes  $IC = 64$ ,  $IC_P = 16$  and therefore Port O is active.

#### D. Schedule-aware Tensor Distribution Network (SDN)

The Schedule-aware Tensor Distribution Network (SDN) serves as the core infrastructure of the proposed FLEXNN accelerator, tasked with efficiently transferring input data between on-chip memory (SRAM) and PE array, and vice versa, adhering to the optimal schedule of the layer [27]. These data include configuration settings, activation and kernel data (IF & FL), sparsity encodings, as well as bias & scale factors essential for the calculation within the PE array. Additionally, the SDN manages the transportation of computational results, including output activation (OF) and partial sums, from the PE array's internal storage structure (RF) back to the SRAM, ensuring that the layout facilitates subsequent tensor layer acceleration. During the operational phases, the input side of the distribution network is termed the “load/fill” phase, while the output side is termed the “drain” phase, as illustrated in Fig. 8.1-2. In fixed hardware accelerators, the pre-determined data layout in SRAM simplifies the load and drain phases, but compromises flexibility and optimization in operations. This rigidity restricts reuse potential, escalates memory accesses, and consequently increases overall energy and power consumption.

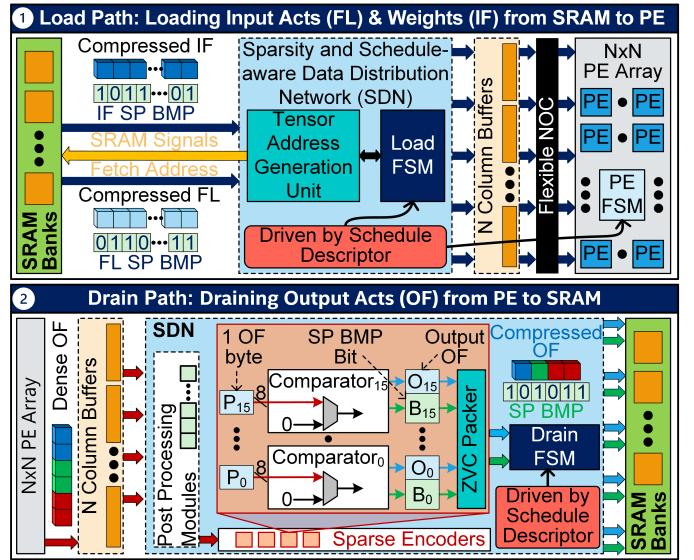


Fig. 8: FLEXNN accelerator load and drain paths. (1) Activations and weights are fetched from SRAM and delivered to PE array. (2) Output activations/partial sums are fetched from PE array and routed to SRAM after compression in Sparse Encoders in SDN. Flexible schedule support is integrated in load and drain FSM.

Flexible hardware demands dynamic changes in the SRAM data layout, contingent on the type of reuse and optimal schedule (blocking and partitioning) for the layer.

The usual design consideration revolves around simplifying one phase, while the other manages the complexities associated with rearranging the data to adhere to the optimal schedule. When the SRAM data layout remains fixed, the loading process must handle the complexity associated with unpacking the fixed layout data and arranging them according to the predetermined order and sequence dictated by the optimal schedule. Furthermore, the loading process must be hierarchical: initially organizing the input in a manner consumable by a column of PEs based on the partitioning factor and then, within the column, determining which input byte corresponds to which PE based on the blocking factor through a series of multiplexers [28], [29]. For activation data, this involves retrieving data from memory in a predetermined order and distributing the IX, IY, and IC in the sequence and quantity specified by the reuse factor of the optimal schedule. Throughout the reuse process, one set of input remains resident, while the other circulates multiple times. Typically, the optimal schedule strives to maximize reuse, thereby reducing the frequency of fetching from SRAM.

For weight data, there exists an opportunity to prearrange the data offline according to the optimal schedule before storing them in the SRAM. This approach simplifies the load process by eliminating the need for data rearrangement during weight distribution. Conversely, in cases where the SRAM's data layout is flexible rather than fixed, the load process is simplified while the drain process is tasked with packing the output activations according to the predetermined order and sequence outlined



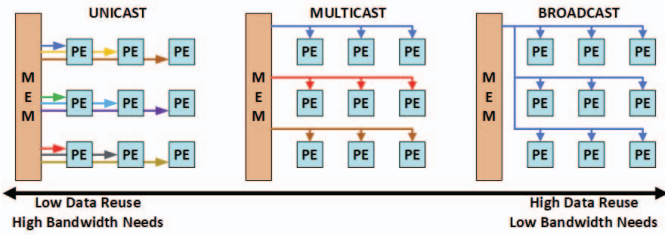


Fig. 9: Data distribution patterns through flexible NoC.

by the optimal schedule. The drain component, responsible for gathering output points from the PE array, must understand the sequence of OX, OY, and OC in which the data are transmitted by the PEs. Then it rearranges or packs them based on the IX, IY, and IC parameters of the optimal schedule for the subsequent layer. However, if the data layout for the load is fixed, the drain only needs to rearrange the output points into a predetermined layout (such as Z-major), regardless of the optimal schedule for the next layer [30]. Another critical aspect of the distribution network is the interconnect or Network-on-Chip (NoC) used to link the PE array with the drain and load blocks in the design. NoC must have the ability to unicast, multicast or broadcast the input data to one or more PEs based on the order specified by the optimal schedule, as demonstrated in Fig. 9. This maximizes reuse and minimizes the number of accesses to SRAM, improving overall efficiency, as defined in existing research [31].

### E. Two-sided Sparsity Acceleration

In the proposed FLEXNN accelerator, our aim is to harness the sparsity in both FLs and IFs to enhance not only energy efficiency but also throughput. Throughout the DNN framework, the data remains compressed until reaching the PE. Operating within the compressed domain offers advantages, such as reducing on-chip bandwidth requirements and storage demands, potentially leading to energy savings and throughput enhancements. However, handling compressed data, which often varies in length, poses challenges in terms of data manipulation, such as distributing data across PEs and implementing sliding window processing within the PE [32]. In this section, we will introduce an innovative two-sided sparsity acceleration logic capable of processing sparse data within the compressed domain to achieve higher throughput [33]–[36].

The core idea is that IFs or FLs with a value of 0 do not contribute to non-zero outcomes during MAC operations, allowing them to be skipped during both the compute and storage phases [37]. The DRAM serves as storage for zero-value compressed input activations and weights, which are delivered to the load module in batches [34], [38]. The load module then transmits the compressed inputs and weights to their respective buffers. Along with these, the load module also transfers the corresponding bitmaps to the input and weight bitmap buffers, respectively. The sparsity acceleration module receives all of these compressed data and bitmaps as input, and through a series of combinational operations, it

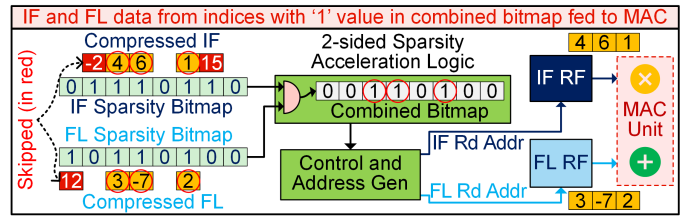


Fig. 10: Two-sided combined sparsity acceleration logic.

determines the exact non-zero values in the inputs and weights that need to be computed in the dot product. These values are then fed into the compute module, which generates the output feature maps. Subsequently, these feature maps are stored in the store module, which incorporates a zero-value compression module to compress the zero-valued elements. These compressed feature maps are then stored back in the DRAM for further processing in subsequent layers of the DNN.

The sparsity acceleration logic partitions the incoming input activations and weights in blocks, and aims to find the participating pairs in the dot product computation, by accounting for the fine grained sparsity. The logic starts off with generating an activation and weight bitmap corresponding to the incoming values. The bitmaps consist of 1-bit values, represented by either ‘0’ or ‘1’, instead of 8-bit values present in the original activation and weight sets (considering an 8-bit quantized network). For every non-zero element in the activation set, the corresponding position in the activation bitmap consists of ‘1’. The bitmap consists of a ‘0’ for every zero value in the activation set. Similarly, the weight bitmap is also obtained from the incoming set of weights. Subsequently, we also obtained a compressed activation and weight set of values, which only consists of non-zero elements in the corresponding original sets. The compressed sets, along with the two bitmaps, are subsequently stored in the memory to be fetched during computation to perform the MAC operation during inference, as demonstrated in Fig. 10.

During the compute phase, the two bitmaps, corresponding to activations and weights, are logically AND-ed to obtain another intermediate bitmap. The total number of 1s in this intermediate bitmap depicts the total number of activation and weight pairs that will result in non-zero partial sums, which must be accumulated over time. Activations and weights at these non-zero positions are provided as input to the PE, significantly reducing compute operations. Through the combined sparsity acceleration logic, our accelerator achieves enhanced computational speed, improving performance, and throughput for DNN inference by exploiting two-sided sparsity. This approach notably decreases the energy consumption of the Processing Element Array, completing tasks with a reduced number of cycles.

## IV. EXPERIMENTAL SETUP

To evaluate the efficiency of the proposed accelerator, we implemented FLEXNN in Chisel 3.0, with the generated RTL simulated in Synopsys VCS®. We chose Chisel because

TABLE I: Comparison of FLEXNN with state-of-the-art fixed schedule accelerator designs. Identical memory hierarchies and cost ratios are used for evaluation.

	Eyeriss [5]	TPU [6]	FLEXNN
<b>Memory Hierarchy</b>	3-level <sup>1</sup>	3-level	3-level
<b>Num of PEs</b>	168	256	256
<b>RF (in each PE)</b>	512 B	32 B	192 B
<b>On-chip Buffer/SRAM<sup>2</sup></b>	108 KB	64 KB	1.5 MB
<b>DRAM</b>	1 GB	28 MB	1 GB
<b>Energy cost ratio (PE:RF:SRAM:DRAM)</b>	1:1:6:200	1:0.06:6:200	1:0.125:6:200

<sup>1</sup>Eyeriss has additional inter-PE communication with RF:PE=1:2 cost ratio <sup>2</sup>SRAM sub-bank size remains constant for all

of its ability to facilitate the generation of parametrizable designs featuring multiple variations of PE, allowing easy modification of RF size, number of MAC units, etc. As mentioned in Section III-A, the accelerator supports *UINT8*, *INT8*, *FP16*, *BF16* precision. Subsequently, the RTL undergoes synthesis in the Synopsys Design Compiler (DC), utilizing one of the industry’s most advanced process technology nodes, (based on 7 nm), to generate the Gate-Level Netlist (GLS) and corresponding area for each accelerator component. To estimate the power consumption within the proposed FLEXNN accelerator, we employed Synopsys Verdi to generate an activity file (Switching Activity Interchange Format: SAIF), using test benches for assistance. The accelerator netlist, coupled with the activity file, serves as input to Synopsys PrimeTimePX (PTPX), enabling power estimation at the gate level for both block and full-chip designs of the FLEXNN accelerator. An overview of this workflow is illustrated in Fig. 11. The FLEXNN architecture comprises a unified tile of 256 PEs organized in a 16x16 grid (16 columns with each column having 16 individual PEs), featuring 8 MAC units within each PE, resulting in a total of 2048 MACs. This tile encompasses 1.5 MB of SRAM equipped with 32-byte read/write ports. The PE consists of 4x16 B IF RF Register File (RF), 4x16 B FL RF, and 16x4 B OF RF, contributing to an overall 192 B RF per PE. The precision of the IF, FL, and OF points is an 8bit integer. The memory hierarchy of our design is illustrated in Table I. Operating at a frequency of 1.8 GHz and 0.75 volts, the accelerator boasts a dense peak Trillion Operations Per Second (TOPS) performance, reaching 7.37 TOPS, with efficiency metrics of 5 TOPS/watt and 4.6 TOPS/mm<sup>2</sup>.

We conducted a comparative analysis of the performance of FLEXNN in conjunction with two state-of-the-art dense accelerators, namely Eyeriss [9] and TPU [13]. The comparison considered various design specifications described in Table I. Furthermore, we evaluated the performance of FLEXNN on sparse DNN workloads using state-of-the-art networks [39]: ResNet50, MobileNetV2, InceptionV3, and GoogLeNet trained on the ImageNet dataset [40]. The first three models were compressed using (i) Quantization-Aware Training (QAT) to quantize weights/activations to INT8 precision and (ii) unstructured pruning using the regularization-based sparsity

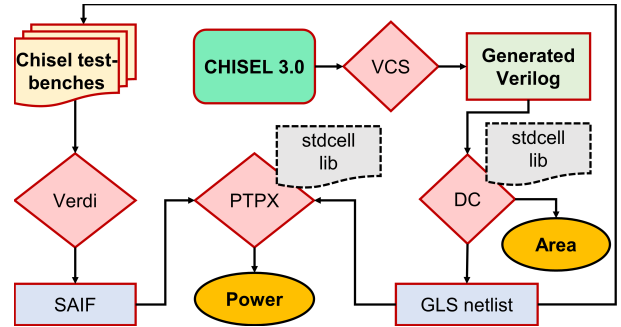


Fig. 11: Workflow overview for FLEXNN implementation. Please refer to text for full-form of abbreviations.

algorithm (RB-sparsity). GoogLeNet was quantized in the same way, but filter pruning with geometric median criterion was applied. The compressed models were obtained from Intel’s Neural Network Compression Framework (NNCF) [41]. Per-layer and overall network weight sparsity were obtained from these models. Furthermore, all models were subjected to inference on the entire ImageNet2012 validation dataset (50,000 images) and activation sparsity at input and output of each layer was calculated using PyTorch hooks. The average activation sparsity across the entire dataset, weight sparsity, and layer statistics were fed into a framework of FLEXNN, which was used to obtain the layer-wise and overall network compute acceleration and total energy consumption of the accelerator, reported in Section V. Specifically, we compared the performance of FLEXNN, which uses two-sided combined sparsity, against dense accelerators without any sparsity support and those capable of exploiting fixed weight-sided sparsity [9], [42]. The framework was modified to evaluate the latency and energy of a dense variant and a weight-sided variant of FLEXNN to allow fair comparison.

## V. EXPERIMENTAL RESULTS

In this section, we begin by providing a breakdown of the power and area consumption for our proposed FLEXNN accelerator. Subsequently, we proceed to evaluate its performance using state-of-the-art network and dataset configurations.

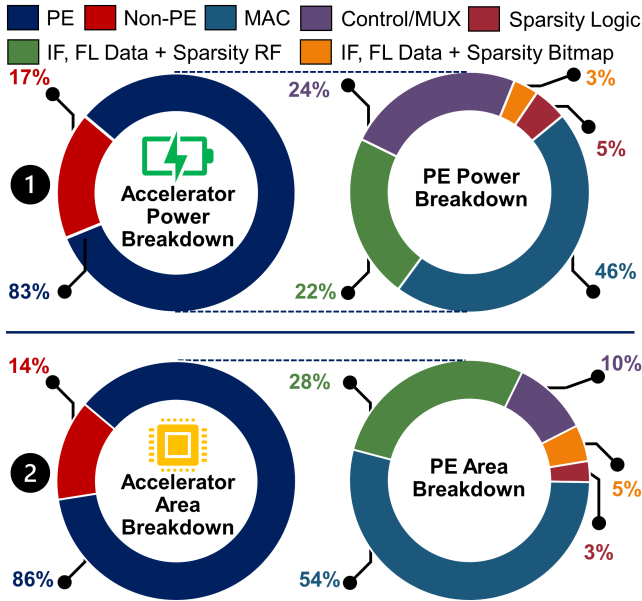


Fig. 12: Area and Power Breakdown of FLEXNN for (1) overall accelerator and (2) PE level granularity.

#### A. FLEXNN Power and Area Results

We assess the power and area cost of the proposed FLEXNN accelerator using an illustrative implementation in this paper. Fig. 12.1 and 2 show the power and area breakdown of the entire accelerator as well as the inter-PE breakdowns, respectively. As shown, the PE array unit consumes  $\approx 83\%$  of power and  $\approx 86\%$  of the total area of the overall accelerator design. Moreover, MAC operation constitutes about 46% of the power and 54% of the area inside each PE of the FLEXNN accelerator. This shows reasonable power and area impact when compared to the significant benefits it provides in terms of the ability to support flexible schedules.

#### B. Comparison with SOTA Fixed Schedule Accelerators

Fig. 13 shows the improvement in energy efficiency of our flexible schedule DNN accelerator FLEXNN over two prominent fixed-schedule designs, Eyeriss [5] and TPU [6] assuming identical memory hierarchies. These results are obtained for two DNNs used in image recognition and object detection, ResNet101 and YOLOv2, using our custom DNN accelerator energy estimation framework. We have used dense models (i.e., with 0 weight sparsity) for these results. Note that we have scaled the memory hierarchy of the two accelerators to the same level as FLEXNN for a fair comparison. In this figure, Here, the y-axis represents a % reduction in energy consumption of FLEXNN compared to these two designs. The left subplot depicts the layer-wise energy reduction for all layers, sorted in increasing order of reduction. In the right subplot, we summarize the distribution of reduction across all layers. The x-axis shows the two comparative accelerators. Compared to Eyeriss, FLEXNN results in 40%–77% reduction for ResNet101 and 45%–77% for YOLOv2. Compared to TPU, FLEXNN provides up to 62% and 58% energy savings for

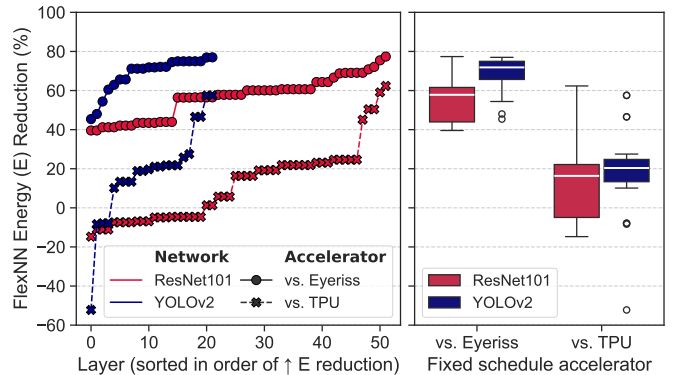


Fig. 13: Layer-wise distribution of % energy improvement of FLEXNN over fixed schedule DNN accelerators (Table I) for ResNet101 and YOLOv2 (dense models). Optimal schedule used for each layer in FLEXNN.

ResNet101 and YOLOv2, respectively. While it is true that in certain layers, FLEXNN exhibits a slight energy increase (indicated by negative energy reduction) compared to TPU, this is primarily attributed to the optimized dataflow on TPU for specific layers, particularly 20 layers in ResNet101 and 4 layers in YOLOv2. However, on average, FLEXNN still provides notable advantages, offering average energy savings of 14% and 22% for these respective DNN architectures over TPU. It is important to note that the heightened energy consumption in these layers stems from the robust support for flexibility within DNN, which inherently introduces slightly higher overhead. On the other hand, we see an average improvement of 57% and 69% over Eyeriss. Despite occasional spikes in energy consumption for select layers, FLEXNN consistently outperforms these fixed-schedule accelerators, showcasing its superior efficiency and overall cost-effectiveness.

#### C. Sparsity Benefits using FLEXNN

In this section, we present a comprehensive analysis of the layer-wise and overall network speed-up achieved by FLEXNN compared to two prominent counterparts: a dense accelerator without any sparsity acceleration support and a fixed weight-sided sparse accelerator. Fig. 14.1–4 presents the layer-wise compute acceleration (y-axis) provided by weight-sided and FLEXNN in comparison with the dense accelerator, for few representative layers (x-axis) of 4 DNN benchmarks. Note that the activation sparsity numbers reported in the following discussion are averaged across the entire dataset. For a fair comparison, benchmarking was performed using the same optimal schedule for all accelerator types.

1) *ResNet50*: The sparse ResNet50 model has 5%–88% unstructured weight sparsity,  $weight\_sp_{layer}$ , resulting in up to 8.1% acceleration across layers in weight-sided accelerator. However, except before the first conv layer, ResNet50 has a high activation sparsity,  $act\_sp_{layer}$ , at the input of every convolution layer due to the presence of the ReLU activation function. On average across the entire ImageNet validation dataset, this amounts to  $act\_sp_{layer} = 14\%$ –83% sparsity.

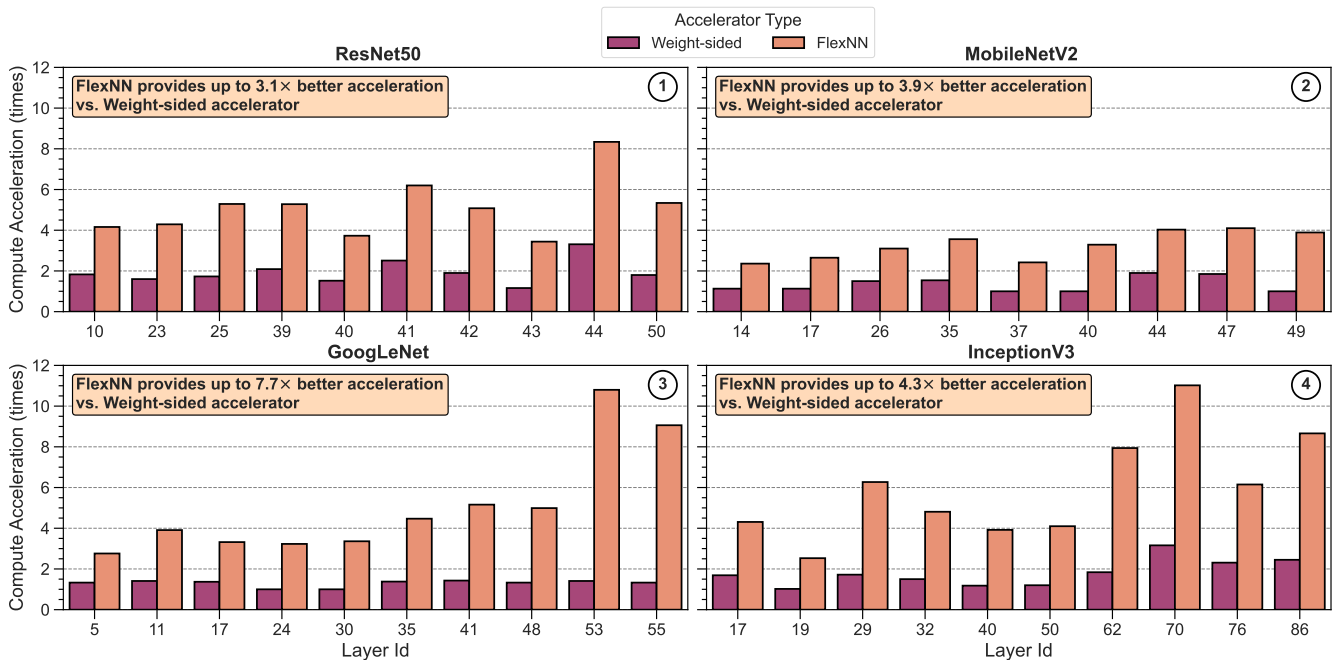


Fig. 14: Comparison of layerwise compute acceleration of FLEXNN and Weight-sided (one-sided) sparse accelerator over dense accelerator (without any sparsity support) benchmarked with (1) ResNet50, (2) MobileNetV2, (3) GoogLeNet, (4) InceptionV3. Only a few representative layers are presented for each network.

FLEXNN conveniently leverages both weight and activation sparsity to provide up to 10.3% compute acceleration, as shown in Fig. 14.1. **Overall, FLEXNN gives up to 3.1× better acceleration than the weight-sided accelerator for ResNet50.**

2) *GoogLeNet*: Since GoogLeNet was filter-pruned, maximum  $weight\_sp_{layer} = 30\%$ . This contributed to maximum 1.4× speed-up in weight-sided accelerator. In contrast, the maximum measured  $act\_sp_{layer} = 91\%$  resulted in a maximum acceleration 10.8× in FLEXNN. **Fig. 14.3 shows that FLEXNN provides up to 7.7× better compute acceleration compared to fixed weight-sided accelerator, even for networks with low weight sparsity.**

3) *InceptionV3*: This model is very sparse with a maximum  $weight\_sp_{layer} = 96\%$ . There are many layers with large dimensions and filter sizes; therefore, both the weight-sided accelerator and FLEXNN can leverage weight sparsity and provide up to 24.7× speed-up for *Mixed.7a.branch3x3.2.conv, Layer Id: 72* (not shown in figure). Although  $act\_sp_{layer}$  for this layer is 78%, FLEXNN cannot provide any additional speed-up for this layer. However, there are many other layers with activation sparsity higher than weight sparsity, allowing FLEXNN to leverage both. As depicted in Fig. 14.4, FLEXNN provides a high level of compute acceleration. Among such layers with sparsity skewed toward activations, the maximum speed-up is 11.3×. Therefore, the proposed design can take the best of both worlds and give better savings than the weight-sided accelerator. **Across all layers, FLEXNN is up to 4.3× faster than the weight-sided accelerator, clearly demonstrating superior performance.**

4) *MobileNetV2*: MobileNetV2 is a compact and lightweight model compared to the other benchmarks discussed earlier. Although sparse MobileNetV2 consists up to 70%  $weight\_sp_{layer}$ , the maximum speed-up provided by the weight-sided accelerator is only 3.3× (last linear layer). Interestingly, the weight sparsity of all conv layers, except *features.18.0, Layer Id: 51* is < 50% leading to a low overall speed-up. However, FLEXNN leveraging activation sparsity (maximum  $act\_sp_{layer} = 74\%$ ) in addition to weights can provide up to 4.1× acceleration. **Fig. 14.2 indicates that even for compact models with small layer sizes, FLEXNN is superior to the weight-sided accelerator by 3.9×.**

5) *Overall Network Acceleration*: The compute acceleration obtained by dense, weight-sided and our proposed accelerator for the entire end-to-end network inference, depicted in Fig. 15 reveal a significant acceleration advantage conferred by FLEXNN across all evaluated networks. Here, the y-axis represents the acceleration, whereas the x-axis represents benchmarks. The dense accelerator does not provide any acceleration as it cannot leverage weight or activation sparsity, denoted by values 1. Evidently, the speed-up for weight-sided accelerator is proportional to the overall network weight sparsity. Across all these networks, the weight-sided accelerator provides 1.2×–1.7× speed-up. On the contrary, the acceleration obtained in FLEXNN is proportional to the relative distribution of weight and activation sparsity. For ResNet50,  $weight\_sp_{network}, act\_sp_{network} = 61\%, 55\%$  and FLEXNN takes advantage of them to provide 2.2× speed-up. MobileNetV2 and GoogLeNet

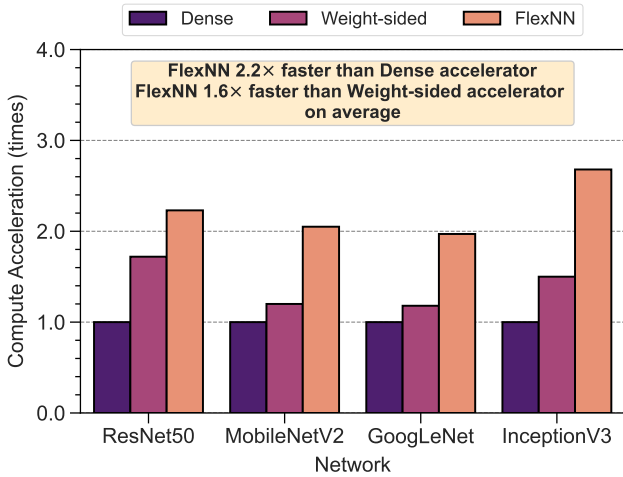


Fig. 15: Comparison of compute acceleration for full network inference in FLEXNN over dense and weight-sided accelerator benchmarked with 4 DNNs.

has  $weight\_spnetwork, act\_spnetwork = 52\%, 30\%$  and  $weight\_spnetwork, act\_spnetwork = 24\%, 58\%$ , respectively. These results in  $2.1\times$  and  $2.0\times$  speed-up, respectively. Clearly, even with these two networks with low sparsity on one side, FLEXNN provides a similar speed-up to ResNet50 due to two-sided sparsity support. Finally, InceptionV3 has  $weight\_spnetwork, act\_spnetwork = 61\%, 63\%$  contributing to  $2.7\times$ , which is the maximum across the 4 networks. As evident from these results, our accelerator consistently outperforms both dense and weight-sided architectures in terms of compute acceleration. **This substantial improvement,  $2.2\times$  vs. dense and  $1.6\times$  vs. weight-sided accelerator (on average), underscores the efficacy of our proposed approach in enhancing overall network speed-up, demonstrating its superiority in accelerating DNN inference computations.** Furthermore, the observed acceleration benefits are valid across the various architectural complexities and model sizes represented by the diverse DNNs considered in our evaluation. This robust performance underscores the versatility and effectiveness of two-sided sparsity acceleration support in FLEXNN across a spectrum of deep learning model architectures.

6) *Energy Efficiency improvement*: Fig. 16 presents the improvement in energy efficiency of 3 different accelerator architectures (y-axis) while evaluating 4 DNN benchmarks (x-axis) on the ImageNet validation dataset. We considered dense accelerator energy consumption as the baseline. As evident from the figure, these results largely correlate with overall network compute acceleration in Fig. 15 since the accelerator circuits are active for a reduced amount of time. Furthermore, compared to the weight-sided accelerator, FLEXNN allows for substantial reduction in memory cycle count as ZVC compressed data flows through the different memory hierarchies, resulting in reduced memory energy consumption. This is enabled by the sparsity-aware load and drain path, as explained in Section III-D. Note that DRAM transactions are not considered in these results.

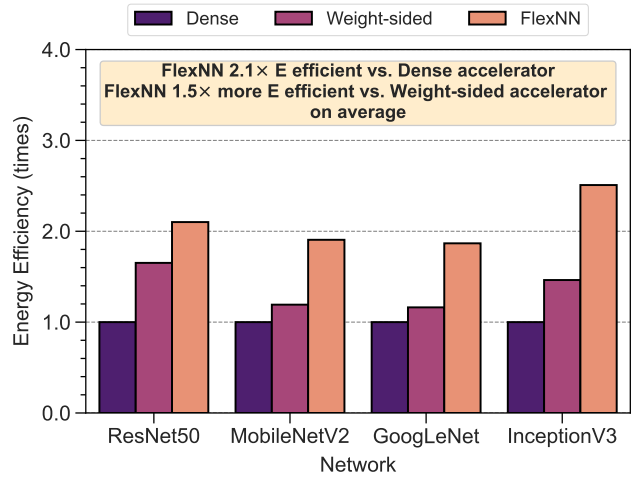


Fig. 16: Comparison of energy efficiency for full network inference in FLEXNN over dense and weight-sided accelerator benchmarked with 4 DNNs.

**Across all 4 benchmarks, FLEXNN is  $2.1\times$  and  $1.5\times$  more energy efficient than the dense and weight-sided accelerators, respectively.**

In conclusion, our comprehensive evaluation showcases not only the substantial compute acceleration achieved by our proposed accelerator, but also its remarkable energy efficiency improvements compared to existing dense and weight-sided architectures. This underscores the pivotal role of our approach in addressing the dual challenges of performance enhancement and energy conservation in DNN accelerators, paving the way for sustainable and efficient AI hardware solutions.

## VI. RELATED WORK

Recent years have witnessed a surge in the field of DNN accelerators. Most DNN accelerator designs only implement fixed schedules with fixed dataflow. Fig. 17 illustrates the different DNN accelerators from industry and academia and their supported datatypes. For example, NeuFlow [43] and ISAAC [44] implement a weight stationary schedule, ShiDianNao [45] and Movidius VPU2 [46] implement an output stationary schedule, Google TPU [6] only implements Nonlocal Reuse schedule, and Eyeriss [5] from MIT implements a row stationary schedule. A key challenge arises from the limitations of the tensor data PE module hardware, which operates solely on a fixed dataflow pattern. It lacks the ability to dynamically adjust to accommodate diverse schedules, as it lacks awareness of any schedule information, owing to its restricted functionality. Therefore, one cannot implement different schedules (i.e. dataflows) in these accelerators, and till today there are no existing accelerators that can support flexible schedules. In addition to hardware solutions, software-based solutions can mimic programmable PE array units that can perform computation on varying dataflow tensor data in general-purpose CPUs and GPUs, but fixed-function accelerators do not support this flexibility in design. Therefore, these software

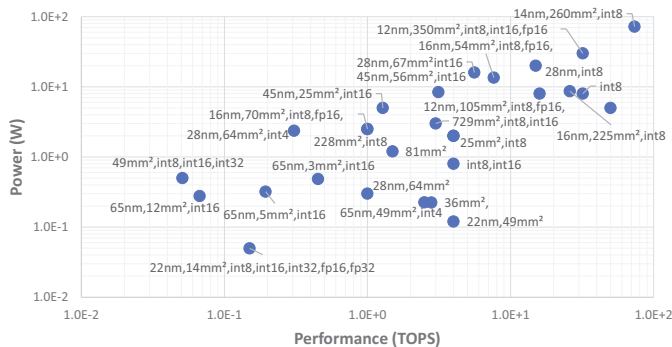


Fig. 17: Edge DNN accelerator competitive landscape, plotted with public data, considering baseline reference [14].

solutions cannot be used in existing accelerators. Moreover, software solutions are far from being energy optimal to be considered for adoption in edge inference devices. FPGAs provide an alternative avenue for DNN acceleration with flexibility, but the hardware configuration of the FPGA cannot be changed during the execution of one DNN application, which also implies a fixed schedule during execution. Additionally, FPGAs have lower energy efficiency compared to ASIC hardware accelerators.

Since the PE array modules in all previous designs have limited functionalities in the form of a basic MAC structure, which is the compute kernel for convolution operation, the wide degree of mismatch between the data patterns required by different input, weight, and output stationary optimal schedules makes it impossible for the fixed architecture PE array to be able to handle the tensor data correctly without sacrificing energy and/or performance. The key disadvantage is that the PE array that performs convolution computation in these previous solutions is not schedule aware. Due to this limitation, reformatting the energy optimal dataflow type into a dataflow that is supported by the underlying fixed architecture PE array induces severe performance and energy penalty as more SRAM reads are required to complete the work and prevents the PE array from reaching maximum utilization if the accesses are serialized. Software solutions can also be used for rearranging the input, output activation as well as weight tensor data for different optimal schedules to be fed into the PE array, into the type of fixed dataflow supported by the PE array, which not only would require assisting CPUs but would also be highly energy and performance inefficient, thereby significantly diminishing the energy efficiency gains offered by flexible scheduling.

In contrast to these approaches, we propose a **schedule-aware runtime configurable PE array module**, which can (1) process tensor data (both weights and activations) that are either input, output, or weight stationary, or even a mixture of these dataflow types, depending upon the energy optimal schedule for the current DNN layer, (2) have its microarchitecture be reconfigurable at runtime based on software-programmable configuration registers, and (3) leverage maximum activation and weight reuse by having small amount of distributed local storage close to compute within the PE array itself. The dataflow

support in the proposed PE array module is flexible. It is controlled by a list of configuration descriptors, which are set at the beginning of the execution of each layer. This tensor data computation PE array module is a pure hardware solution that exposes hardware knobs to the compiler and configures the dataflow during runtime, enabling the flexible schedules of convolutional layers in DNN accelerators without performance penalty due to rearranging computation within the PE or having to offload any work to CPU or software.

## VII. CONCLUSION

In this paper, we proposed a flexible schedule-aware DNN accelerator FLEXNN, which can adapt its internal dataflow to the optimal schedule of each layer in DNNs. Our proposed solution maximizes data reuse at each memory level, resulting in significant energy savings arising from optimal data reuse. Note that flexibility works seamlessly on top of existing performance-enhancing features such as sparsity acceleration and low-precision logic, and it does not diminish their impact in any manner. It is evident that this flexibility comes at the cost of additional area overhead compared to fixed dataflow accelerators, but it also enables us to achieve significant energy savings on average across a myriad of DNN layers. Furthermore, we propose a novel approach to improve throughput and reduce energy usage in the FLEXNN architecture. Taking advantage of fine-grained sparsity in both activation and weight tensors, we optimize the inference engine within the hardware accelerator. Experimental results demonstrate significant improvements in both performance and energy efficiency compared to existing DNN accelerators. This research contributes to ongoing efforts to develop more efficient hardware accelerators for executing deep neural networks.

## VIII. ACKNOWLEDGEMENTS

We would like to sincerely thank Gautham China, Debebrata Mohapatra, Huichu Liu, Moongon Jung, Sang Kyun Kim, Guruguhanathan Venkataramanan, Raymond Sung, Hong Wang, and Cormac Brick for their contributions to this work.

## REFERENCES

- [1] A. Raha, R. Sung, S. Ghosh, P. K. Gupta, D. A. Mathaikutty, U. I. Cheema, K. Hyland, C. Brick, and V. Raghunathan, "Efficient hardware acceleration of emerging neural networks for embedded machine learning: An industry perspective," in *Embedded Machine Learning for Cyber-Physical, IoT, and Edge Computing: Hardware Architectures*. Springer, 2023, pp. 121–172.
- [2] A. Raha, S. K. Kim, D. A. Mathaikutty, G. Venkataramanan, D. Mohapatra, R. Sung, C. Brick, and G. N. China, "Design considerations for edge neural network accelerators: An industry perspective," in *2021 34th International Conference on VLSI Design and 2021 20th International Conference on Embedded Systems (VLSID)*. IEEE, 2021, pp. 328–333.
- [3] S. K. Ghosh, A. Raha, and V. Raghunathan, "Energy-efficient approximate edge inference systems," *ACM Transactions on Embedded Computing Systems*, vol. 22, no. 4, pp. 1–50, 2023.
- [4] A. Raha, S. Ghosh, D. Mohapatra, D. A. Mathaikutty, R. Sung, C. Brick, and V. Raghunathan, "Special session: Approximate tinyml systems: Full system approximations for extreme energy-efficiency in intelligent edge devices," in *2021 IEEE 39th International Conference on Computer Design (ICCD)*. IEEE, 2021, pp. 13–16.

- [5] Y.-H. Chen, J. Emer, and V. Sze, "Eyeriss: A spatial architecture for energy-efficient dataflow for convolutional neural networks," in *Proceedings of the 43rd International Symposium on Computer Architecture*, ser. ISCA '16, 2016.
- [6] N. P. Jouppi et al., "In-datacenter performance analysis of a tensor processing unit," 2017.
- [7] H. Kwon, P. Chatarasi, M. Pellauer, A. Parashar, V. Sarkar, and T. Krishna, "Understanding reuse, performance, and hardware cost of dnn dataflow: A data-centric approach," in *Proc. MICRO*, ser. MICRO '52. New York, NY, USA: Association for Computing Machinery, 2019, p. 754–768.
- [8] Y.-H. Chen, J. Emer, and V. Sze, "Eyeriss: A spatial architecture for energy-efficient dataflow for convolutional neural networks," *ACM SIGARCH computer architecture news*, vol. 44, no. 3, pp. 367–379, 2016.
- [9] Y.-H. Chen, T. Krishna, J. S. Emer, and V. Sze, "Eyeriss: An energy-efficient reconfigurable accelerator for deep convolutional neural networks," *IEEE journal of solid-state circuits*, vol. 52, no. 1, pp. 127–138, 2016.
- [10] A. Parashar, M. Rhu, A. Mukkara, A. Puglielli, R. Venkatesan, B. Khailany, J. Emer, S. W. Keckler, and W. J. Dally, "Scnn: An accelerator for compressed-sparse convolutional neural networks," *ACM SIGARCH computer architecture news*, vol. 45, no. 2, pp. 27–40, 2017.
- [11] S. K. Ghosh, S. Kundu, A. Raha, D. A. Mathaikutty, and V. Raghunathan, "Harvest: Towards efficient sparse dnn accelerators using programmable thresholds," in *2024 37th International Conference on VLSI Design and 2021 20th International Conference on Embedded Systems (VLSID)*. IEEE, 2024.
- [12] Chen *et al.*, "Eyeriss v2: A flexible accelerator for emerging deep neural networks on mobile devices," *IEEE Journal on Emerging and Selected Topics in Circuits and Systems*, vol. 9, no. 2, pp. 292–308, 2019.
- [13] N. P. Jouppi, C. Young, N. Patil, D. Patterson, G. Agrawal, R. Bajwa, S. Bates, S. Bhatia, N. Boden, A. Borchers *et al.*, "In-datacenter performance analysis of a tensor processing unit," in *Proceedings of the 44th annual international symposium on computer architecture*, 2017, pp. 1–12.
- [14] M. Horowitz, "1.1 Computing's energy problem (and what we can do about it)," in *Proc. ISSCC*, 2014.
- [15] T. Hoefler, D. Alistarh, T. Ben-Nun, N. Dryden, and A. Peste, "Sparsity in deep learning: Pruning and growth for efficient inference and training in neural networks," *JMLR*, vol. 22, no. 1, pp. 10882–11005, 2021.
- [16] J. Albericio, P. Judd, T. Hetherington, T. Aamodt, N. E. Jerger, and A. Moshovos, "Cnvlutin: Ineffectual-neuron-free deep neural network computing," *ACM SIGARCH Computer Architecture News*, vol. 44, no. 3, pp. 1–13, 2016.
- [17] S. Zhang, Z. Du, L. Zhang, H. Lan, S. Liu, L. Li, Q. Guo, T. Chen, and Y. Chen, "Cambricon-x: An accelerator for sparse neural networks," in *2016 49th Annual IEEE/ACM International Symposium on Microarchitecture (MICRO)*. IEEE, 2016, pp. 1–12.
- [18] S. Han, X. Liu, H. Mao, J. Pu, A. Pedram, M. A. Horowitz, and W. J. Dally, "Eie: Efficient inference engine on compressed deep neural network," *ACM SIGARCH Computer Architecture News*, vol. 44, no. 3, pp. 243–254, 2016.
- [19] X. Yang, M. Gao, Q. Liu, J. Setter, J. Pu, A. Nayak, S. Bell, K. Cao, H. Ha, P. Raina *et al.*, "Interstellar: Using halide's scheduling language to analyze dnn accelerators," in *Proceedings of the Twenty-Fifth International Conference on Architectural Support for Programming Languages and Operating Systems*, 2020, pp. 369–383.
- [20] H. Kwon, P. Chatarasi, V. Sarkar, T. Krishna, M. Pellauer, and A. Parashar, "Maestro: A data-centric approach to understand reuse, performance, and hardware cost of dnn mappings," *IEEE micro*, vol. 40, no. 3, pp. 20–29, 2020.
- [21] D. Mohapatra, A. Raha, G. China, H. Liu, C. Brick, and L. Hacking, "Configurable processor element arrays for implementing convolutional neural networks," Apr. 30 2020, uS Patent App. 16/726,709.
- [22] S. Hsu, A. Agarwal, D. Mohapatra, A. Raha, M. Jung, G. China, and R. Krishnamurthy, "Multi-buffered register files with shared access circuits," Apr. 22 2021, uS Patent App. 17/132,895.
- [23] A. Raha, D. Mohapatra, G. China, G. Venkataramanan, S. K. Kim, D. Mathaikutty, R. Sung, and C. Brick, "Performance scaling for dataflow deep neural network hardware accelerators," Sep. 2 2021, uS Patent App. 17/246,341.
- [24] D. Mohapatra, A. Raha, D. A. Mathaikutty, R. J.-H. Sung, and C. M. Brick, "Runtime configurable register files for artificial intelligence workloads," Mar. 10 2022, uS Patent App. 17/530,156.
- [25] D. Mohapatra, A. Raha, D. Mathaikutty, R. Sung, and C. Brick, "Schedule-aware dynamically reconfigurable adder tree architecture for partial sum accumulation in machine learning accelerators," Apr. 28 2022, uS Patent App. 17/520,281.
- [26] A. Raha, M. A. Anders, R. J.-H. Sung, D. Mohapatra, D. A. Mathaikutty, R. K. Krishnamurthy, and H. Kaul, "Floating point multiply-accumulate unit for deep learning," Jun. 16 2022, uS Patent App. 17/688,131.
- [27] G. China, H. Liu, A. Raha, D. Mohapatra, C. Brick, and L. Hacking, "Schedule-aware tensor distribution module," Feb. 20 2024, uS Patent 11,907,827.
- [28] D. Mathaikutty, A. Raha, R. Sung, D. Mohapatra, and C. Brick, "Sparsity-aware datastore for inference processing in deep neural network architectures," Mar. 3 2022, uS Patent App. 17/524,333.
- [29] D. A. Mathaikutty, A. Raha, R. J.-H. Sung, and D. Mohapatra, "Data reuse in deep learning," Jun. 16 2022, uS Patent App. 17/684,764.
- [30] A. Raha, D. A. Mathaikutty, U. I. Cheema, and D. Kondru, "Output drain path facilitating flexible schedule-based deep neural network accelerator," Jan. 11 2024, uS Patent App. 18/474,464.
- [31] H. Kwon, A. Samajdar, and T. Krishna, "Maeri: Enabling flexible dataflow mapping over dnn accelerators via reconfigurable interconnects," *ACM SIGPLAN Notices*, vol. 53, no. 2, pp. 461–475, 2018.
- [32] A. Raha, D. Mohapatra, D. A. Mathaikutty, R. J.-H. Sung, and C. M. Brick, "System and method for balancing sparsity in weights for accelerating deep neural networks," Mar. 17 2022, uS Patent App. 17/534,976.
- [33] G. China, D. Mathaikutty, G. Venkataramanan, D. Mohapatra, M. Jung, S. K. Kim, A. Raha, and C. Brick, "Accelerated loading of unstructured sparse data in machine learning architectures," Feb. 11 2021, uS Patent App. 17/081,509.
- [34] A. Raha, D. Mathaikutty, D. Mohapatra, S. K. Kim, G. China, and C. Brick, "Methods and apparatus to load data within a machine learning accelerator," Oct. 21 2021, uS Patent App. 17/359,392.
- [35] A. Raha, M. Langhammer, D. Mohapatra, N. Tunali, and M. Wu, "Methods and apparatus to perform low overhead sparsity acceleration logic for multi-precision dataflow in deep neural network accelerators," Sep. 15 2022, uS Patent App. 17/709,337.
- [36] S. Kundu, A. Raha, D. A. Mathaikutty, and K. Basu, "Rash: Reliable deep learning acceleration using sparsity-based hardware," in *2024 25th International Symposium on Quality Electronic Design (ISQED)*. IEEE, 2024.
- [37] F. Connor, D. Bernard, and N. Hanrahan, "Dot product calculators and methods of operating the same," U.S. Patent 10,768,895 B2, Sep. 8, 2020.
- [38] G. China, D. Mohapatra, A. Raha, H. Liu, and C. Brick, "Methods, systems, articles of manufacture, and apparatus to decode zero-value-compression data vectors," Oct. 31 2023, uS Patent 11,804,851.
- [39] M. AI, "The latest in machine learning — papers with code," <https://paperswithcode.com/>.
- [40] A. Krizhevsky, I. Sutskever, and G. E. Hinton, "Imagenet classification with deep convolutional neural networks," *Advances in neural information processing systems*, vol. 25, 2012.
- [41] A. Kozlov, I. Lazarevich, V. Shamporov, N. Lyalyushkin, and Y. Gorbachev, "Neural network compression framework for fast model inference," *arXiv preprint arXiv:2002.08679*, 2020.
- [42] J. Park, H. Yoon, D. Ahn, J. Choi, and J.-J. Kim, "Optimus: Optimized matrix multiplication structure for transformer neural network accelerator," *Proceedings of Machine Learning and Systems*, vol. 2, pp. 363–378, 2020.
- [43] C. Farabet, B. Martini, B. Corda, P. Akselrod, E. Culurciello, and Y. LeCun, "Neuflow: A runtime reconfigurable dataflow processor for vision," in *CVPR 2011 WORKSHOPS*, 2011, pp. 109–116.
- [44] A. Shafiee, A. Nag, N. Muralimanohar, R. Balasubramonian, J. P. Strachan, M. Hu, R. S. Williams, and V. Srikumar, "Isaac: A convolutional neural network accelerator with in-situ analog arithmetic in crossbars," in *2016 ACM/IEEE 43rd Annual International Symposium on Computer Architecture (ISCA)*, 2016, pp. 14–26.
- [45] Z. Du, R. Fasthuber, T. Chen, P. Ienne, L. Li, T. Luo, X. Feng, Y. Chen, and O. Temam, "Shidiannao: Shifting vision processing closer to the sensor," in *2015 ACM/IEEE 42nd Annual International Symposium on Computer Architecture (ISCA)*, 2015, pp. 92–104.
- [46] Intel, "Intel keembay," <https://newsroom.intel.com/wp-content/uploads/sites/11/2019/11/intel-ai-summit-keynote-slides.pdf>.